9.8 Velocity and Pressure Maps Above a Transonic Delta Wing

Contributed by:
R. Konrath, C. Klein

The parallel application of experimental diagnostics methods allows a more complete description of complex flow phenomena and provides high quality data for validation of numerical calculations. As an example the parallel application of the Pressure Sensitive Paint (PSP) technique and PIV shall be presented. Such investigations have been performed in the frame of the Inter-

Table 9.13. PIV recording parameters for combined velocity and pressure measurements on a delta wing.

Flow condition	$Ma = 0.4 / Re_{MAC} = 3 \cdot 10^6$
Maximum in-plane velocity	$U_{\max} = 200\,\mathrm{m/s}$
Interrogation volume	$146 \times 60 \times 294\ mm^{-3}$ $(H \times W \times D)$
Dynamic spatial range	DSR ≈ 30
Dynamic velocity range	DVR ≈ 80
Observation distance	$z_0 = 0.6\,\mathrm{m}$
Recording method	multi frame, single exposure
Recording medium	PCO SensiCam QE, 1376×1024 pixel
Recording lens	$f = 60.0$, $f_\# = 5.6$
Illumination	Nd:YAG laser[a], 300 mJ/pulse
Pulse delay	$\Delta t = 4\,\mu\mathrm{s}$
Seeding material	DEHS droplets ($d_\mathrm{p} = 1\mu$)

[a] frequency doubled

national Vortex Flow Experiment 2 (VFE-2), where wind tunnel tests were carried out on a 65° delta wing at sub- and transonic speeds applying both techniques. Since 2003 the VFE-2 is being carried out within the framework of the task group AVT-113 of RTO (NATO's Research and Technology Organization). The objectives of this working group are to perform new wind-tunnel tests on a delta wing by using modern measurement techniques and to compare these data with results of numerical state-of-the-art codes [326]. For the tests, the delta wing model, provided by NASA Langley, was equipped with sharp as well as with rounded leading edges.

With PSP the pressure distributions on the model surface measurements were determined, which serve as "pathfinder" tests. Their results gave first information of the flow topology over the delta-wing for a large range of angles of attack. The PIV measurements were performed in a second test campaign for which specific angles of attack and locations of the measurement planes above the delta wing were selected on the basis of a first analysis of the PSP results. The measured velocity fields provide detailed information of the instantaneous and time averaged flow fields.

The stereo-PIV setup (see figure 9.44) allows for flow velocity measurements above the delta wing within planes perpendicular to the model axis at different chord stations. The light-sheet and the cameras can be translated along the model axis during wind tunnel operation. The arrangement also incorporates rotary plates in order to adjust quickly the setup for different angles of attack.

For the current delta wing configuration, a specific flow topology occurs in the rounded leading edge case. In addition to the well known outer primary vortex another inner primary vortex develops which was first evidenced within the VFE-2 group for $M = 0.4$, $R_{MAC} = 3 \cdot 10^6$ (w.r.t. mean aerodynamic chord) and an angle of attack of 13° by a flow computation of FRITZ (EADS-Munich, see [326]). This computation was invoked by the PSP results

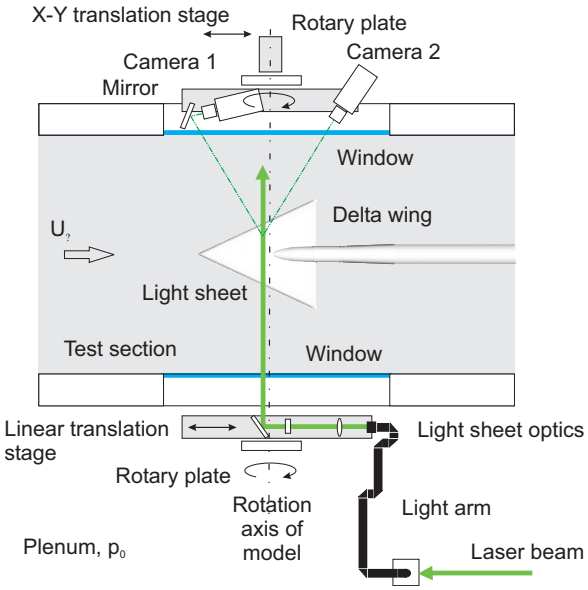

Fig. 9.44. Stereoscopic PIV arrangement inside the perforated test section of the transonic wind tunnel DNW-TWG showing the coated delta-wing and light sheet.

and used the measured pressure distributions to set up simulation parameters. The PIV results obtained later agree with the computed flow topology. The flow topology can be seen in figure 9.45 showing the measured pressured distribution on the model surface together with the measured velocity and vorticity distributions in planes of the different chord stations. In this case the flow separates at the leading edge first at $x/c_r = 0.5$ and the primary vortex is formed, which produces a strong suction peak in the pressure distributions. However, another weaker suction peak can be detected more inboard with a highest peak height just downstream the origin of the outer primary vortex. The velocity distributions at $x/c_r = 0.6$ reveal that this suction peak is produced by another inner vortex co-rotating to the outer one. This vortex develops from a thin vortex structure which occurs more upstream close to the surface, i.e. $x/c_r = 0.4$. Instantaneous PIV results show [327] that this vortex structure consists of several small co-rotating vortices spreading in the spanwise direction. Between the outer primary vortex and the inner vortical structure the flow re-attaches to the surface and separates again so that vortices of the inner vortical structure detach from the surface, i.e. $x/c_r = 0.5$. These vortices merge and a circular inner vortex is formed such that two co-rotating vortices of approximately the same size can be observed at $x/c_r = 0.6$. Further downstream vorticity is fed only into the outer primary vortex and the strength of the inner vortex gradually decreases, whereas the inner and the outer vortex remain separated and do not merge.

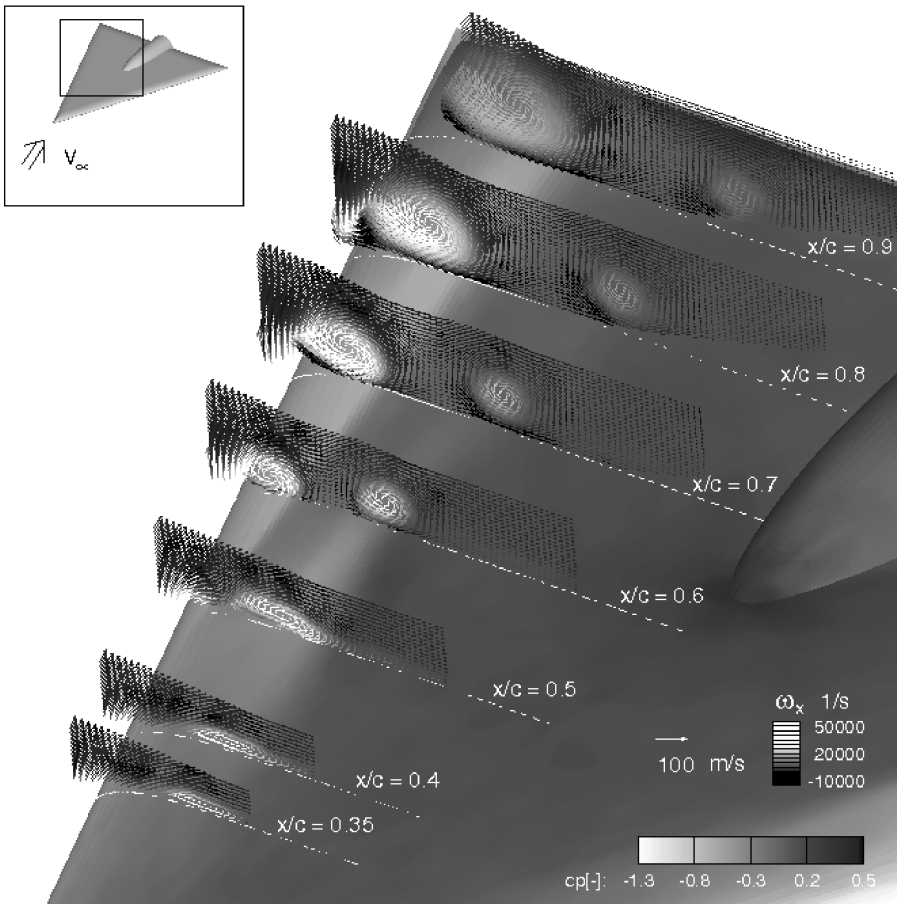

Fig. 9.45. Time averaged pressure, velocity and vorticity distributions above the delta wing with rounded leading edges for $\alpha = 13.3°$, $Ma = 0.4$ and $R_{MAC} = 3 \cdot 10^6$. The in-plane velocity vectors are plotted in different planes perpendicular to the delta wing axis. The gray levels of the vectors correspond to the out-of-plane vorticity. The gray levels at the surface are related to the local pressure coefficient.